RSC Advances

PAPER

View Article Online
View Journal | View Issue

Cite this: *RSC Adv.*, 2016, **6**, 69509

Near-infrared luminescence of Nd^{3+} and Yb^{3+} complexes using a polyfluorinated pyrene-based β-diketonate ligand†

T. M. George,[ab] S. Varughese[b] and M. L. P. Reddy*[ab]

A new polyfluorinated β-diketonate ligand containing a pyrene chromophore, namely, 4,4,5,5,6,6,6-heptafluoro-3-hydroxy-1-(pyren-1-yl)hex-2-en-1-one (Hhfpyr) has been designed and employed for the development of a series of near-infrared (NIR) emitting lanthanide complexes (Nd^{3+} and Yb^{3+}) in the absence and presence of an ancillary ligand, 4,7-diphenyl-1,10-phenanthroline (bath). The isolated NIR-emitting lanthanide complexes [$Nd(hfpyr)_3(H_2O)$ **1**, $Nd(hfpyr)_3(bath)$ **2**, $Yb(hfpyr)_3(H_2O)$ **3** and $Yb(hfpyr)_3(bath)$ **4**] have been characterized by various spectroscopic techniques and evaluated their photoluminescence properties. The photophysical properties disclosed that the developed pyrene-based β-diketonate ligand is well suited for the sensitization of Nd^{3+} as well as Yb^{3+} emissions, thanks to the favourable position of the triplet state (T^1) of the ligand ($\Delta E = T^1 - {}^4F_{3/2} = 4700\ cm^{-1}$ for Nd^{3+} and $\Delta E = T^1 - {}^2F_{5/2} = 6200\ cm^{-1}$ for Nd^{3+}), as evidenced from the phosphorescence spectra of the corresponding Gd^{3+} complexes. Most importantly, the displacement of solvent molecules from the coordination sphere of the NIR emitting lanthanide binary complexes (**1** and **3**) with an ancillary ligand markedly enhances the quantum yields ($\Phi_{overall} = 0.45$ for **1** to 1.07% for **2** and from 1.69 for **3** to 3.08% for **4**) and excited state lifetime values ($\tau = 2.80$ for **1** to 6.16 μs for **2** and from 6.88 for **3** to 13.45 μs for **4**). Notably, Yb^{3+} ternary compound **4** with promising NIR luminescence properties was embedded into PMMA matrices, giving rise to a series of PMMA-supported hybrid materials (PMMA@**4**), where the thermal stability and the film-forming properties were significantly enhanced.

Received 11th May 2016
Accepted 17th July 2016

DOI: 10.1039/c6ra12220e

www.rsc.org/advances

Introduction

Near-infrared (NIR) luminescence, especially from lanthanide complexes such as Nd^{3+} and Yb^{3+} has emerged as an area of paramount interest due to its pioneering technological applications in fields ranging from bioimaging to optical communications.[1] However, since f–f transitions are parity forbidden, unligated Ln^{3+} ions have strikingly low molar absorption coefficients and hence direct excitation of lanthanide ions always leads to modest luminescence intensities.[2] As a consequence, many efforts have been made in order to enhance the absorption coefficients of Ln^{3+} ions and thereby achieved efficient photoluminescence.[3] Fortunately, this objective can be easily realized by prudent selection of new antenna chromophores with suitable conjugated motifs.[4] In this context, β-diketonates are particularly important because such ligands can efficiently absorb ultraviolet light and transfer the absorbed energy to the central Ln^{3+} ions in an appropriately effective manner.[4c,5] Indeed, there exists an absolute challenge to design and develop a novel β-diketonate ligand with relatively low triplet energy level, which matches well with the first excited state of NIR luminescent Ln^{3+} ions[1a,6] ($^4F_{3/2}$ for $Nd^{3+} = 11\ 257\ cm^{-1}$ or $^2F_{5/2}$ for $Yb^{3+} = 10\ 400\ cm^{-1}$) as compared with visible luminescent Ln^{3+} ions having relatively high first excited state energy levels ($^5D_0$ for $Eu^{3+} = 17\ 286\ cm^{-1}$ or $^5D_4$ for $Tb^{3+} = 20\ 545\ cm^{-1}$). Recently, some feasible strategies have been proposed by many researchers to improve the NIR luminescence of Ln^{3+} ions.[7] For example, the fluorination of the β-diketonate ligand for minimizing the non-radiative decay pathways or molecular engineering of the β-diketonate ligand with appended suitable extended π-conjugated chromophore moieties to achieve efficient sensitization of the NIR luminescence of Ln^{3+} ions.[8] Also, the replacement of coordinated solvent molecules around the central Ln^{3+} ion with an appropriate ancillary ligand, avoids the quenching effects due to the presence of high-frequency oscillators.[9] Bünzli and co-workers has reported a new antenna molecule containing four benzoyltrifluoroacetone moieties anchored to single carbon atom and connected through four flexible methoxy groups namely as a sensitizer for NIR emitting

[a]AcSIR-Academy of Scientific & Innovative Research, CSIR-NIIST Campus, Thiruvananthapuram, India

[b]Materials Science and Technology Division, National Institute for Interdisciplinary Science and Technology (NIIST), Council of Scientific and Industrial Research (CSIR), Thiruvananthapuram-695 019, India. E-mail: mlpreddy55@gmail.com

† Electronic supplementary information (ESI) available. CCDC 1473942. For ESI and crystallographic data in CIF or other electronic format see DOI: 10.1039/c6ra12220e

lanthanides.[10] New bis-β-diketonate ligand by coupling two mono-diketonate ligands (2-theonyltrifluoroacetone) has also been proposed for the sensitization of Yb^{3+} ions with higher quantum yields as compared with the mononuclear analogue.[11]

Pyrene, a well-known organic hydrocarbon was extensively employed as a fluorophore of choice in the field of photochemistry and photophysics.[12] In addition, some of the pyrene-derivatives have been used in Organic Light Emitting Diodes intending to improve the hole transporting ability because of its electron-rich property.[13] There are also a few reported examples that use pyrene as a sensitizer for lanthanide emission. The 'antenna effect' in europium complexes involving a pyrene-based triacid ligand was first disclosed by Fages *et al.*[14] Later, near-IR emission was noted in ytterbium and neodymium complexes containing a pyrene chromophore linked to a macrocycle *via* different tether lengths.[15] In the later studies, Pope reported Yb^{3+}, Nd^{3+} and Er^{3+} complexes with two pyrene chromophores tethered by a diethylene triaminepentaacetic acid chelate.[16] These investigations have inspired us to develop a new antenna ligand for the sensitization of Nd^{3+} and Yb^{3+} ions by anchoring a pyrene chromophore to the β-diketonate ligand (Fig. 1).

It is well documented that the NIR-emitting Ln^{3+} ions are especially inclined to vibrational deactivation.[9] Organic chromophores containing high-energy oscillators, such as C–H and O–H bonds are able to quench the Ln^{3+} excited states non-radiatively, thus exhibiting weak luminescence intensities and shorter excited-state lifetimes. The replacement of C–H bonds with C–F bonds is an important strategy for the design and development of novel Ln^{3+} complexes with efficient photophysical properties.[7h,17] As per the earlier literature reports, the replacement of C–H bonds in a β-diketonate ligand with low energy C–F oscillators is able to lower the vibrational energy of the ligand and thereby enhances the emission intensity of the Ln^{3+} ion.[18] In addition, due to heavy atom effect, which facilitate the intersystem crossing and as a result the lanthanide-centered luminescent properties are improved.[19] Therefore in the present work, a new β-diketonate molecule, namely, 4,4,5,5,6,6,6-heptafluoro-3-hydroxy-1-(pyren-1-yl)hex-2-en-1-one (Hhfpyr) has been designed by simultaneously incorporating pyrene moiety as well as heptafluorinated alkyl chain. The developed β-diketonate ligand has been utilized for the construction of a series of lanthanide complexes (Ln^{3+} = Nd, Yb and Gd) in the absence and presence of an ancillary ligand, 4,7-diphenyl-1,10-phenanthroline. The synthesized lanthanide complexes were characterized by various spectroscopic techniques and evaluated their photophysical properties.

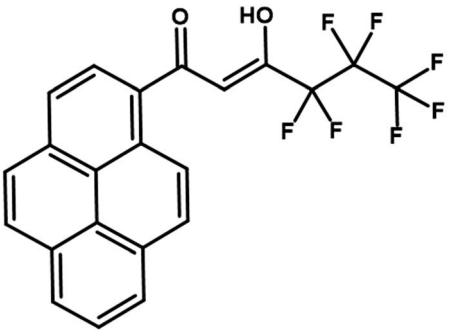

Fig. 1 Structure of the ligand Hhfpyr.

Nevertheless, NIR emitting Ln^{3+}–β-diketonate complexes typically exhibit low thermal-stability, limited photostability and poor mechanical properties. These inherent limitations hinder the practical application of NIR emitters in many of the optoelectronic technologies. It is well-known that the blending of luminescent near-IR emitting Ln^{3+} compounds in polymeric materials renders a series of advantages for the development of molecular materials, for instance, thermal, chemical and mechanical stability, biocompatibility and the photoluminescence properties.[6a,7e,20] To the best of our knowledge, there are only few examples in the literature dealing with the incorporation of NIR emitting ternary-β-diketonate complexes into the PMMA materials.[6c,21] Hence in the present study the newly developed luminescent NIR emitting Yb^{3+} complex has been incorporated into a host polymer matrix, such as poly(-methyl methacrylate) films and investigated their photoluminescence behaviour.

Experimental

Materials and characterization

Ytterbium(III) nitrate hexahydrate (99.99%), neodymium(III) nitrate hexahydrate (99.99%), gadolinium(III) nitrate hexahydrate (99.99%), lanthanum(III) nitrate hexahydrate (99.99%), 1-acetylpyrene (97%), ethyl perfluorobutyrate (97%), sodium hydride (60% dispersion in mineral oil), poly(methyl methacrylate) (98%) and bathophenanthroline (97%) were purchased from Sigma-Aldrich and used without further purification. All the other chemicals employed were of analytical reagent grade.

Single-crystal XRD data for complex **2** were collected with a Rigaku Saturn 724+ diffractometer using graphite-monochromated Mo Kα radiation, and the data were processed using Rigaku Crystal Clear software. The molecular structure of the complex was solved and refined by the SHELXTL suite of programs.[22]

Elemental analyses were carried out on Elementar – vario MICRO cube elemental analyzer. A Perkin-Elmer Spectrum two FT-IR spectrometer was used to record the infra-red spectral data and a Bruker Avance II 500 MHz NMR spectrometer was used to record the ^{1}H NMR (500 MHz) and ^{13}C NMR (125.7 MHz) spectra with tetramethylsilane as the internal standard. The electrospray ionization (ESI) mass spectra were measured with a Thermo Scientific Exactive Benchtop LC/MS Orbitrap Mass Spectrometer. The thermogravimetric analyses were performed on a TG/DTA-6200 (SII Nano Technology Inc., Japan). The optical spectra of the synthesized ligand and its corresponding metal complexes were recorded with a Shimadzu UV-3600 UV-vis spectrophotometer.

Photophysical measurements were carried out in the solid state at room temperature. Emission spectra were obtained with an Edinburgh FLS 980 spectrofluorometer equipped with a 450 W xenon arc lamp. Emission spectra were corrected for source intensity (lamp and grating) and emission spectral response (detector and grating) by standard correction curves. The

absolute fluorescence quantum yields were measured on an Edinburgh FLS 980 steady state spectrometer using an integrating sphere. Luminescent excited state lifetimes in the range from 0.5 ns to 50 μs were measured by an Edinburgh FLS 980 spectrofluorometer equipped with a digital oscilloscope (Tektronix) for data acquisition in time-correlated single-photon counting experiments with a pulsed microsecond xenon flash-lamp. The estimated experimental errors are 2 nm on the photoluminescence bands maxima, 5% on the luminescence quantum yield. The lifetime measurements carried out at low temperature using a Spex 1040D phosphorimeter.

Synthesis of the ligand 4,4,5,5,6,6,6-heptafluoro-3-hydroxy-1-(pyren-2-yl)hex-2-en-1-one (Hhfpyr)

The new β-diketonate ligand (Hhfpyr) was prepared according to a modified Claisen condensation method as detailed in Scheme 1. 1-Acetylpyrene (1.0 mmol) and ethyl perfluorobutyrate (1.0 mmol) were dissolved in dry tetrahydrofuran (25 mL) and the resultant mixture was stirred for 15 min in an ice bath at 0 °C. To this reaction mixture, sodium hydride (2.0 mmol) was added dropwise in nitrogen atmosphere and stirred for 20 min, followed by further stirring for 12 h at 70 °C. To the above reaction mixture, 40 mL of 2 M HCl was added and extracted twice into dichloromethane (2 × 30 mL). Then the organic layer was collected and dried over Na_2SO_4, and the solvent was removed by evaporation. The product obtained was then purified by column chromatography on silica gel with a solvent mixture consisting of hexane and ethyl acetate (10 : 1) as an eluent. Yield: 80%. Elemental analysis (%): calculated for $C_{22}H_{11}F_7O_2$ (440.06): C 60.01, H 2.52; found: C 60.23, H 2.63. ^{1}H NMR ($CDCl_3$, 500 MHz) δ (ppm): 15.53 (broad, enol–OH), 8.78 (d, 1H, J = 9 Hz), 8.23 (m, 6H), 8.05 (m, 2H), 6.62 (s, 1H). ^{13}C NMR (125.7 MHz, $CDCl_3$) δ (ppm): 190.58, 176.78, 134.71, 131.14, 130.51, 130.21, 129.90, 128.09, 127.05, 126.78, 126.70, 126.64, 126.55, 125.01, 124.38, 125.01, 124.38, 124.26, 124.11, 99.48, 77.16–76.05 ($CDCl_3$). FT-IR (KBr) ν_{max} (cm^{-1}): 3427 (O–H), 1596, 1508, 1346, 1226, 1069, 962, 898, 763, 680, 539. m/z = 463.05 $(M + Na)^+$.

Synthesis of complexes Ln(hfpyr)$_3$(H$_2$O) [Ln = Nd (1), Yb (3) and Gd (5)]

To a methanolic solution of Hhfpyr (12 mmol), 12 mmol of NaOH in water was added and stirred for 5 min. $Ln(NO_3)_3 \cdot 6(H_2O)$ in 3 mL of water (4 mmol) was added drop-wise to the above reaction mixture and stirred for 24 h at 298 K (Scheme 2). The resultant crude precipitate was filtered, washed with water and dried. The obtained metal complex was recrystallized from chloroform solution.

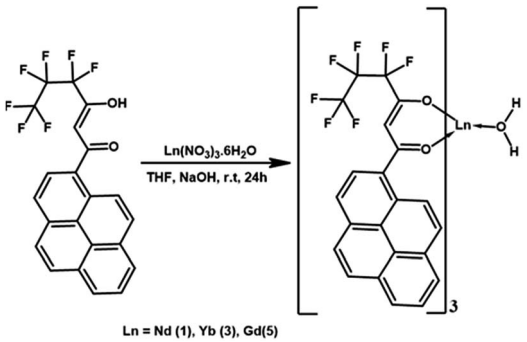

Scheme 2 Synthesis of the Ln^{3+} (Ln = Nd, Yb and Gd) binary complexes.

Nd(hfpyr)$_3$(H$_2$O) (1). Elemental analysis (%): calculated for $C_{66}H_{32}F_{21}O_8Nd$ (1480.16): C 53.56, H 2.18; found: C 53.35, H 2.27. FT-IR (KBr) ν_{max} (cm^{-1}): 3434, 1609, 1514, 1344, 1226, 1153, 1068, 1028, 968, 846, 742, 681, 536. m/z = 1462.09 $[Nd(hfpyr)_3 + 1]^+$.

Yb(hfpyr)$_3$(H$_2$O) (3). Elemental analysis (%): calculated for $C_{66}H_{32}F_{21}O_8Yb$ (1508.98): C 52.53, H 2.14; found: C 52.39, H 2.28. FT-IR (KBr) ν_{max} (cm^{-1}): 3435, 1610, 1514, 1345, 1233, 1179, 1032, 971, 849, 746, 685, 540. m/z = 1492.11 $[Yb(hfpyr)_3 + 1]^+$.

Gd(hfpyr)$_3$(H$_2$O) (5). Elemental analysis (%): calculated for $C_{66}H_{32}F_{21}O_8Gd$ (1493.19): C 53.09, H 2.16; found: C 53.29, H 2.28. FT-IR (KBr) ν_{max} (cm^{-1}): 3436, 1607, 1516, 1345, 1232, 1179, 1031, 970, 850, 745, 682, 539. m/z = 1494.11 $[Gd(hfpyr)_3(H_2O)]^+$.

Synthesis of Ln^{3+} ternary complexes Ln(hfpyr)$_3$(bath) [Ln = Nd (2), Yb (4)]

The ternary Ln^{3+} compounds were synthesized by mixing equimolar solutions of the corresponding binary complexes and an ancillary ligand; bathophenanthroline (bath) in $CHCl_3$ solution and the resultant mixture was stirred for 12 h at 70 °C. The metal complexes were then isolated after the removal of solvent by evaporation process. Finally, the ternary lanthanide complexes were obtained by recrystallization from chloroform solution (as described in Scheme 3).

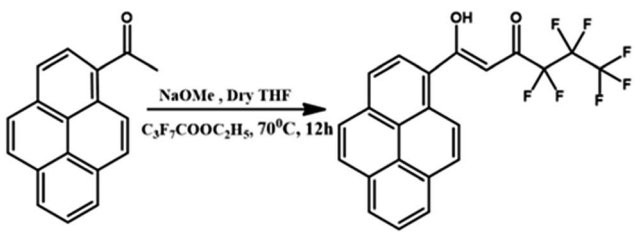

Scheme 1 Synthetic procedure for the ligand Hhfpyr.

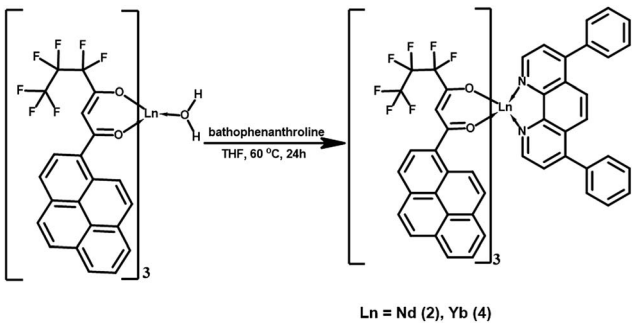

Scheme 3 Synthesis of the Ln^{3+} (Ln = Nd, Yb) ternary complexes.

Nd(hfpyr)$_3$(bath) (2). Elemental analysis (%): calculated for $C_{90}H_{46}F_{21}N_2O_8Nd$ (1794.55): C 60.24, H 2.58, N 1.56; found: C 60.35, H 2.39, N 1.52. FT-IR (KBr) ν_{max} (cm^{-1}): 3028, 1608, 1538, 1513, 1477, 1342, 1225, 1152, 1032, 970, 846, 792, 624, 540. m/z = 1794.22 [Nd(hfpyr)$_3$(bath)]$^+$.

Yb(hfpyr)$_3$(bath) (4). Elemental analysis (%): calculated for $C_{90}H_{46}F_{21}N_2O_8Yb$ (1823.36): C 59.28, H 2.54, N 1.54; found: C 59.37, H 2.39, N 1.56. FT-IR (KBr) ν_{max} (cm^{-1}): 3047, 1609, 1541, 1515, 1477, 1344, 1224, 1156, 1031, 963, 848, 789, 630, 536. m/z = 1384.18 [Yb(hfpyr)$_2$(bath)]$^+$.

Synthesis of Yb^{3+} complex doped PMMA polymer films

The PMMA polymer was doped with the Yb^{3+} complex **4** in the proportions 1, 3, 5, 7 and 9% (w/w). The PMMA powder was dissolved in chloroform, followed by addition of the required amount of complex **4** in chloroform solution, and the respective mixture was heated at 40 °C for 35 min. The polymer films were then obtained after evaporation of excess solvent at 60 °C.

Results and discussion

Synthesis and characterization of the Hhfpyr ligand and Ln^{3+} complexes 1–5

The β-diketonate ligand 4,4,5,5,6,6,6-heptafluoro-3-hydroxy-1-(pyren-1-yl)hex-2-en-1-one (Hhfpyr) was synthesized in 80% yield by a modified Claisen condensation reaction of 1-acetylpyrene with the ethylperfluorobutyrate ester in the presence of sodium hydride in THF medium. The corresponding one pot synthesis of the ligand is described in Scheme 1. The developed ligand has been characterized by the ^{1}H NMR, ^{13}C NMR, FT-IR and electron spray ionisation mass spectroscopic (ESI-MS) methods (Fig. S1–S3 and S9 in the ESI†) as well as by elemental analysis. The developed β-diketonate ligand mainly exists as enol form in $CDCl_3$ solution, as evident from the ^{1}H NMR spectrum of the compound. In the ^{1}H NMR spectrum of Hhfpyr, a broad peak at δ 15.64 ppm corresponding to enolic –OH has been noted. Further, the absence of methyne protons at δ 3.70 ppm confirms the existence of the ligand in enolic form. The synthesis routines for Ln^{3+} binary and ternary complexes are detailed in Schemes 2 and 3, respectively. The elemental analyses and ESI-MS studies (Fig. S4–S8 in the ESI†) of Ln^{3+} complexes (**1–5**) revealed that the central lanthanide ion is coordinating to three β-diketonate ligands. On the other hand, in the case of Ln^{3+} ternary complexes (**2** and **4**), one molecule of the bidentate nitrogen donor, 4,7-diphenyl-1,10-phenanthroline (bath), is also present in the coordination sphere. The FT-IR spectra of the binary Ln^{3+} complexes (**1**, **3** and **5**) display a broad absorption in the 3000–3500 cm^{-1} region, thereby illustrating the presence of water molecule in the coordination sphere of the metal ions (Fig. S10, S12 and S14 in the ESI†). The absence of this broad band in the case of ternary Nd^{3+} and Yb^{3+} complexes (**2** and **4**) inferred that the water molecule is successfully displaced by the bidentate bathophenanthroline ligand (Fig. S11 and S13 in the ESI†). The carbonyl stretching frequency (C=O) of free ligand Hhfpyr (1596 cm^{-1}) was shifted to higher wave numbers in complexes **1–5** (1609 cm^{-1} for **1**; 1610 cm^{-1} for **2**; 1607 cm^{-1} for **3**; 1608 cm^{-1} for **4**; 1609 cm^{-1} for **5**) demonstrating the involvement of carbonyl oxygen in the complex formation with the Ln^{3+} ion. The bands assigned to bathophenanthroline ring stretching modes C=N and C=C can be observed in the 1540–1500 cm^{-1} range and in the 1030–1000 cm^{-1} range, respectively. These bands are shifted in comparison with that of free ancillary ligand, suggesting that bathophenanthroline is coordinating to Ln^{3+} ion.

To further understand the coordination behaviour of the ligands with the lanthanide ions, in the current study, antiparamagnetic lanthanum complexes have been synthesized and characterized by various spectroscopic techniques (experimental procedure and characterizations are given in the ESI†). The ^{1}H NMR spectrum (Fig. S15 in the ESI†) of the lanthanum binary β-diketonate complex, La(hfpyr)$_3$(H_2O) is consistent with the presence of three Hhfpyr units coordinated to the lanthanide ion. The signal for methine proton (–CH) of Hhfpyr appears at 6.51 ppm (δ) and the aromatic protons of the pyrene moiety resonates in the range 8.49 to 7.02 ppm (δ). The upfield shift of the β-diketonate resonances, in the complex, substantiates coordination of ligands with the lanthanide ion. The proton signals of the coordinated water molecule with the metal ion can be noted at 2.59 ppm (δ). In the ternary lanthanum complex, La(hfpyr)$_3$(bath), the methine proton appears at 6.48 ppm (δ). The signals due to aromatic protons of pyrene and bathophenanthroline moiety appear in the range 9.57 to 6.78 ppm (δ) (Fig. S16 in the ESI†). The proton signals appeared in the ternary complex indicates the presence of three Hhfpyr units and one bathophenanthroline moiety in the coordinated complex. Further, no signals for coordinated water molecule noted in the La(hfpyr)$_3$(bath), which indicates the displacement of a coordinated water molecule with the ancillary ligand in the corresponding ternary complex.

The thermal behaviour of Nd^{3+} and Yb^{3+} β-diketonate complexes (**1–5**) was evaluated by means of thermogravimetric analysis (TGA) under nitrogen atmosphere and the results are given in Fig. S21–S24 in the ESI.† It is clear from the TGA data that the complexes **1**, **3** and **5** undergo mass loss approximately 1.19% (calcd: 1.20%) in the first step upto 160 °C, corresponding to the elimination of coordinated water molecule. On the other hand, in the case of ternary Ln^{3+} complexes (**2** and **4**), no weight loss was noted in the range of 120–160 °C, which indicates that these complexes exist as anhydrous in nature. The above results are in accordance with the FT-IR spectral data. The weight loss noted in the thermal analyses of these complexes is found to be much lower than the calculated value for the non-volatile lanthanide oxide, indicating the partial sublimation of these compounds under atmospheric pressure which is well documented in many of the lanthanide fluorinated complexes.[5b,23]

X-ray crystal structure of 3

Slow diffusion of hexane into a solution of the Yb^{3+} binary β-diketonate complex in methanol resulted in the growth of single crystals of **3**. However, our efforts to grow single-crystals of the other Ln^{3+} complexes were not fruitful. The molecular structure

of the Yb^{3+}-pyrene anchored β-diketonate complex (**3**) obtained by X-ray single-crystal diffraction technique is shown in Fig. 2. The pertinent data collection parameters and a list of significant bond distances and angles are presented in Tables 1 and 2, respectively. Yb^{3+} binary β-diketonate complex was found to crystallize in the triclinic crystal system with a $P\bar{1}$ space group. The structure reveals that the Yb^{3+} center adopts a distorted-trigonal prismatic coordination geometry, comprising of three β-diketonate ligands and one solvent water molecule. These results are in good agreement with the crystal structure of tris(acetylacetonato)aquoytterbium reported elsewhere.[24] In general, most of the lanthanide–β-diketonate complexes are eight-coordinated and the coordination sphere features three bidentate β-diketonate ligands and two solvent molecules.[5a] Unusually in the present study, the binary Yb-β-diketonate complex is seven-coordinated and the coordination sphere consisting of three bidentate β-diketonate ligands and one water molecule. This can be attributed to the presence of three bulky conjugated pyrene appended β-diketonate ligands in the coordination sphere of the metal ion, which may sterically hinders the presence of water molecule. The average metal–oxygen distance (2.245 Å) of the β-diketonate ligands is found to be shorter than of the coordinated water molecule (2.298 Å). This observation could be attributed to the presence of a formal negative charge on the β-diketonate oxygen atoms which could enhance the binding to the Yb^{3+} cation due to electrostatic effects.[5a,25] Further, it is interesting to note that one of the metal–oxygen distance of the β-diketonate ligand is surprisingly larger (Yb1–O(7) = 2.298 Å) as compared to the remaining metal–oxygen distances of the β-diketonates [Yb1–O(2) = 2.269 Å; Yb1–O(3) = 2.235 Å; Yb1–O(4) = 2.221 Å; Yb1–O(5) = 2.213 Å; Yb1–O(6) = 2.233 Å]. This may be due to the strong intermolecular hydrogen bonding formation between the coordinated water molecule of Yb1 and one of the β-diketonate oxygen atom coordinated to the neighbouring metal centre as shown in Fig. 3

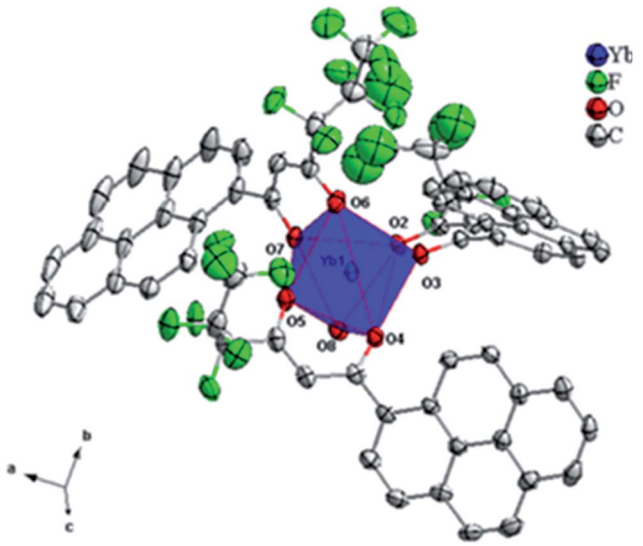

Fig. 2 ORTEP diagram of $[Yb(hfpyr)_3(H_2O)]$ **3** with the thermal ellipsoids drawn at 30% probability level and the hydrogen atoms removed for clarity.

Table 1 Crystallographic and refinement data for **3**

Formula	$C_{66}H_{32}F_{21}O_7Yb$
Formula weight	1508.96
Crystal system	Triclinic
Space group	$P\bar{1}$
Crystallite size (mm^3)	0.20 × 0.20 × 0.15
Temperature (K)	123 K
a (Å)	14.204(3)
b (Å)	15.184(3)
c (Å)	17.459(4)
α (deg)	113.56(1)
β (deg)	108.085(15)
γ (deg)	94.308(12)
V ($Å^3$)	3194.2(12)
Z	2
D_{calcd} (g cm^{-1})	1.569
μ (Mo Kα) (mm^{-1})	1.577
$F(000)$	1486.0
R_1 [$I > 2\sigma(I)$]	0.0606
wR_2 [$I > 2\sigma(I)$]	0.1638
R_1 (all data)	0.0677
wR_2 (all data)	0.1696
GOF	1.178
CCDC	1473942

Table 2 Selected bond lengths (Å) and angles (°) for complex **3**

Bond lengths (Å)		Bond angles (°)	
Yb1–O2	2.2685	O5–Yb1–O4	75.928
Yb1–O3	2.2352	O3–Yb1–O2	75.222
Yb1–O4	2.2209	O3–Yb1–O7	139.825
Yb1–O5	2.2130	O2–Yb1–O8	80.475
Yb1–O6	2.2335	O6–Yb1–O8	153.723
Yb1–O7	2.2980	O5–Yb1–O6	88.143
Yb1–O8	2.2980	O4–Yb1–O3	73.531

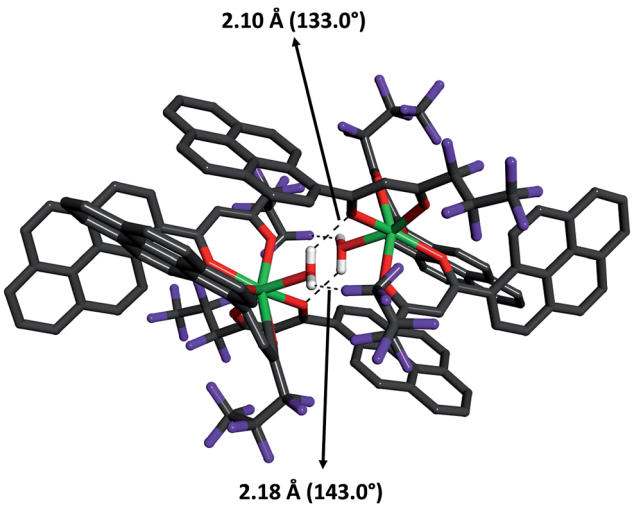

Fig. 3 Intermolecular hydrogen bond present in **3** between water oxygen atoms and β-diketonate oxygen and fluorine atoms of Hhfpyr (shown with broken lines).

[the O–H···O (H···O distance = 2.10 Å) with an angle of 133.0° falls within the typical range hydrogen bonding interactions].[25] In addition, there also exists a strong intermolecular hydrogen bonding interaction between the coordinated water molecule and the fluorine atom of the β-diketonate ligand coordinated to the adjacent Yb1 centre [O–H···F (H···F = 2.18 Å) with an angle of 143.0°]. These intermolecular interactions combine to form an interesting dimeric unit between the two coordinated metal centres.

Optical spectra of the Ln^{3+} complexes

The room-temperature optical spectra of the ligands and the corresponding Nd^{3+} and Yb^{3+} complexes (**1–4**) recorded in THF solution ($c = 1 \times 10^{-5}$ M) are shown in Fig. 4 and 5 respectively. The spectral shapes of the complexes are similar to that of the free Hhfpyr, indicating that the coordination of Ln^{3+} ion does not have significant influence on the energy of the singlet state of the β-diketonate. The ligand displays a composite broad band in the wavelength region 325–475 nm (λ_{max} = 370 nm), which can be assigned to the singlet–singlet n–π* enolic transition of the β-diketonate. In addition, a high energy absorption band noted in the region 275–325 nm can be attributed to the π–π* transition of the aromatic moiety of the β-diketonate. The molar absorption coefficient (ε) of the developed β-diketonate ligand was found to be 15 800 L mol^{-1} cm^{-1} at λ_{max} = 370 nm, which highlights that the β-diketonate ligand has an ability to absorb light. The magnitudes of the molar absorption coefficient values of Nd^{3+} complexes **1** (ε = 49 800 L mol^{-1} cm^{-1} at λ_{max} = 370 nm) and **2** (ε = 50 200 L mol^{-1} cm^{-1} at λ_{max} = 370 nm) were found to be approximately three-fold higher than that of the β-diketonate ligand. This is in consistent with the presence of three β-diketonate ligands in the respective complexes as observed from the elemental analysis data. Similar trends have been noticed in the case of Yb^{3+} complexes **3** (ε = 49 500 L mol^{-1} cm^{-1} at λ_{max} = 370 nm) and **4** (ε = 49 300 L mol^{-1} cm^{-1}).

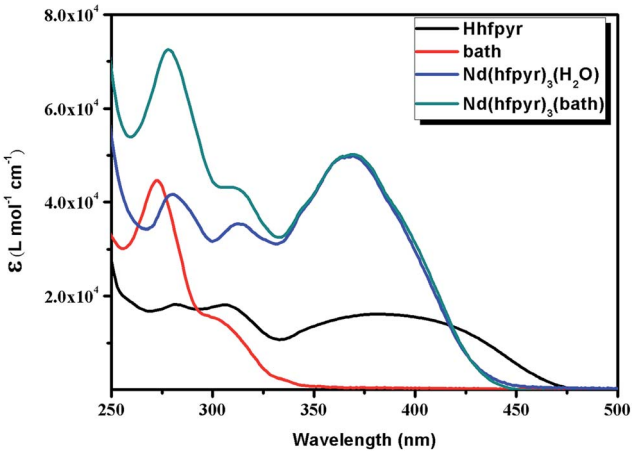

Fig. 4 UV-vis absorption spectra of the ligands Hhfpyr, bath and complexes **1** and **2** in THF ($c = 1 \times 10^{-5}$ M) solution at 298 K.

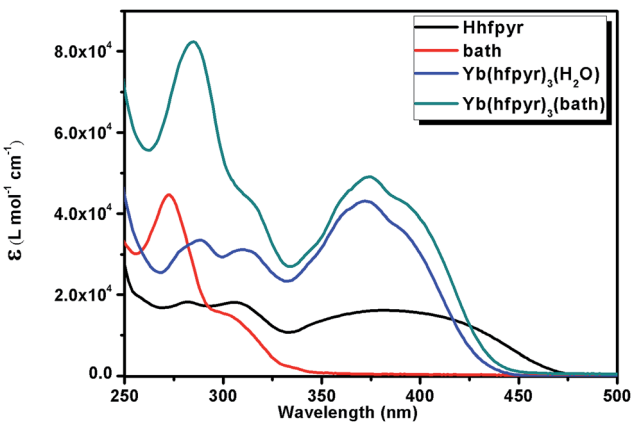

Fig. 5 UV-vis absorption spectra of the ligands Hhfpyr, bath and complexes **3** and **4** in THF ($c = 1 \times 10^{-5}$ M) solution at 298 K.

Photophysical properties

NIR luminescent Nd^{3+} and Yb^{3+} complexes possess considerable promise for practical applications, as their photophysical properties have several distinct advantages over organic fluorophores and semiconductor nanoparticles.[1c] For near-infrared Ln^{3+}, their lowest excited states, and their ground states are primarily close in their energy, and hence, the emission often occurs in the infrared region and their intensities are weaker by several orders of magnitude, compared to that of visible light emitting Ln^{3+} ions.[8c] Moreover, their deactivation process often occurs easily through a non-radiative transition. Therefore, a fundamental challenge is to develop an appropriate antenna molecule for the sensitization of the near-infrared lanthanide ions. Thus, in the current study, a new β-diketonate molecule has been developed by anchoring pyrene as a chromophore group.

To understand the energy transfer processes in the newly isolated NIR emitting Nd^{3+} and Yb^{3+} β-diketonate complexes, it is necessary to determine the singlet (S^1) and triplet (T^1) energy levels of the synthesized new β-diketonate ligand. The singlet energy level of the ligand was determined by reference to the UV-vis upper absorption edge of the $Gd(hfpyr)_3(H_2O)$ **5** (Fig. 6), and the value was found to be 22 935 cm^{-1} (436 nm).[26] The triplet energy level of the β-diketonate ligand was determined by referring to the lower wavelength emission edge from the low-temperature phosphorescence spectrum of (Fig. 6) the $Gd(hfpyr)_3(H_2O)$ **5**.[27] The efficient ligand-to-metal energy transfer requires a good intersystem-crossing efficiency, which is maximized when the energy difference between singlet and triplet states, ΔE (S^1–T^1), is closed to 5000 cm^{-1} as coined by Reinhoudt's empirical rule.[28] In the present system, it amounts to 6728 cm^{-1}, and therefore the newly developed β-diketonate ligand exhibits a good intersystem-crossing efficiency. It is well recognized that the Gd^{3+} complexes are a popular choice for elucidating the triplet energy level of a newly developed antenna molecule due to the following reason: (i) the first excited state energy levels of Gd^{3+} are situated at high energies (^5I_J = 36 900 cm^{-1}), and hence there is no Gd^{3+} emission in the visible region and all the emissions noted is due to the ligand part of the complex. Therefore, the lower emission edge of the 77 K

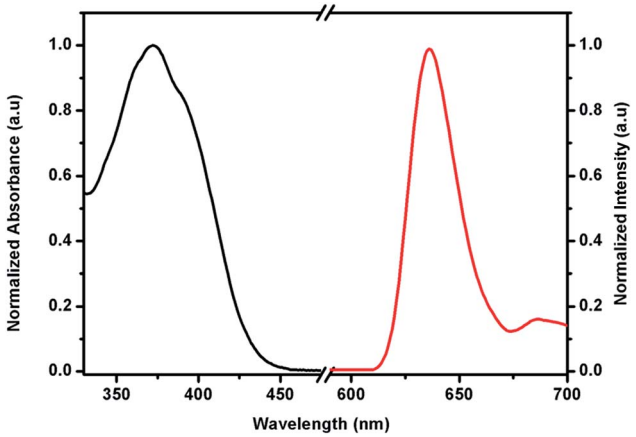

Fig. 6 UV-vis absorption spectrum at 298 K (black) and 77 K phosphorescence spectra (red) of the Gd(hfpyr)$_3$(H$_2$O) complex.

phosphorescence spectrum of the Gd^{3+} complex designates the triplet energy level of the ligand.[27] Thus the triplet energy level of the developed β-diketonate ligand ($T^1 = 16\ 207\ cm^{-1}$ 617 nm) lie well above the energy of the main emitting level of $^4F_{3/2}$ for Nd^{3+} (11 257 cm^{-1}) or $^2F_{5/2}$ for Yb^{3+} (10 400 cm^{-1}), implying that the developed β-diketonate ligand can act as an efficient antenna molecule for the sensitization of both trivalent Nd^{3+} or Yb^{3+} ions. The room-temperature lifetime experiment of Gd(hfpyr)$_3$(H$_2$O) shows that the decay curve can be fitted to a bi-exponential decay with $\tau_1 = 1.58$ ns and $\tau_2 = 6.66$ ns (Fig. S25 in the ESI†). This indicates that the main energy transfer in the present complexes may be through the triplet state of the ligand.[29] The long lifetime value (typically 522 μs) measured for Gd(hfpyr)$_3$(H$_2$O) at 77 K is consistent with the emission from characteristic triplet state (Fig. S26 in the ESI†).[30]

The excitation and emission profiles for the Nd^{3+} complexes (**1** and **2**) in the solid state at room temperature are depicted in Fig. 7. The excitation spectra of these complexes monitored around the intense $^4F_{3/2} \rightarrow {}^4I_{11/2}$ transition (1068 nm) of the Nd^{3+} ion consist of a broad band in the region 250–500 nm (λ_{ex} = 400 nm) and several weak intra-configurational f–f transitions (Fig. 7). The broad band is due to the excitation of the organic chromophores (Hhfpyr and bath) and the weak intraconfigurational f–f transitions originating from the ground state of the Nd^{3+} ion. The f–f transitions could be assigned to $^4I_{9/2} \rightarrow {}^2K_{15/2}$, $^4G_{9/2}$, $^2(D,P)_{3/2}$, $^4G_{11/2}$ (509 nm), $^4I_{9/2} \rightarrow {}^4G_{9/2}$, $^4G_{7/2}$, $^2K_{13/2}$ (528 nm), and $^4I_{9/2} \rightarrow {}^4G_{5/2}$, $^2G_{7/2}$ (584 nm).[8g] However, these f–f transitions are weaker than the absorption of the organic ligands, which proves that the luminescence sensitization *via* excitation of the pyrene-based polyfluorinated-β-diketonate ligand is efficient. Moreover, the excitation spectra of these complexes show a good overlap with ligand-centred ππ* absorption band of the complex which reflects that energy transfer takes place from ligands to Nd^{3+} ion (antenna effect).

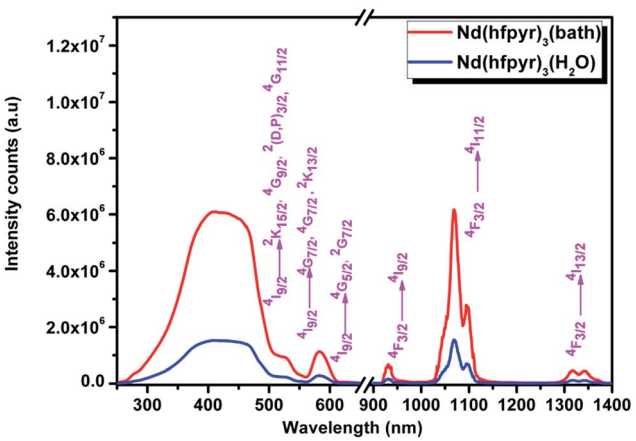

Fig. 7 Room temperature excitation and emission spectra of complexes **1** and **2** in the solid-state.

Under the ligand excitation (λ_{ex} = 400 nm), the emission spectra of the Nd^{3+} complexes (**1** and **2**) exhibit characteristic sharp bands of the Nd^{3+} ion in the range 850–1400 nm spectral range (Fig. 7). The emission spectra essentially display three emission peaks that are assigned to $^4F_{3/2} \rightarrow {}^4I_{9/2}$ (891 nm), $^4F_{3/2} \rightarrow {}^4I_{11/2}$ (1068 nm) and $^4F_{3/2} \rightarrow {}^4I_{13/2}$ (1331 nm).[31] It is interesting to note that some crystal field fine structure can be observed from the emission profiles of these complexes, which illustrates that the Nd^{3+} ion occupies well-defined crystallographic sites in the complexes. Among these transitions, the intensity of the $^4F_{3/2} \rightarrow {}^4I_{11/2}$ transition is strongest, which has potential application in laser systems.[1a] On the other hand, the longer emission wavelength line of Nd^{3+} ($^4F_{3/2} \rightarrow {}^4I_{13/2}$) at 1331 nm may find applications in the development of new optical amplification materials for telecommunications.[1a] Further, a moderate residual ligand emission has been observed in Nd^{3+} binary complex (Fig. S27 in ESI†). On the other hand, negligible residual ligand emission can be noted from ternary Nd^{3+} compound. The results demonstrated that the displacement of a water molecule in the coordination sphere of the Nd^{3+} in Nd(hfpyr)$_3$(H$_2$O) by an ancillary ligand, 4,7-diphenyl-1,10-phenanthroline remarkably enhances (4-fold) the emission intensity of the transition $^4F_{3/2} \rightarrow {}^4I_{11/2}$.

The solid-state room temperature (298 K) excitation spectra of Yb^{3+} complexes (**3** and **4**) obtained by monitoring the characteristic emission of the Yb^{3+} ion at 979 nm are given in Fig. 8. The excitation profiles are dominated by a broad band ranging from 250–550 nm for both the binary and ternary complexes. This broad band can be accredited to the absorption of the organic chromophores (Hhfpyr and bath) employed for the synthesis of the Yb^{3+} ion complexes. The emission spectra of the Yb^{3+} complexes derived from pyrene-based β-diketonate ligand (**3** and **4**), upon ligand-mediated excitation at 400 nm, clearly shows the characteristic emission bands for Yb^{3+} ion at 979 nm, which are assigned to $^2F_{5/2} \rightarrow {}^2F_{7/2}$ transition.[31d,e] Further, it can be noted that the primary emission band of Yb^{3+} ion has been split into an envelope of bands arising at the lower energy side (1006 nm and 1033 nm). These spectral features can be attributed to the splitting of the emitting levels as a consequence of ligand field effects.[32] The emission intensity at 979 nm of Yb^{3+} ternary complex (**4**) has been significantly enhanced (about three fold) as compared to Yb^{3+} binary complex (**2**). Accordingly, negligible residual ligand emission has been noted in Yb^{3+}

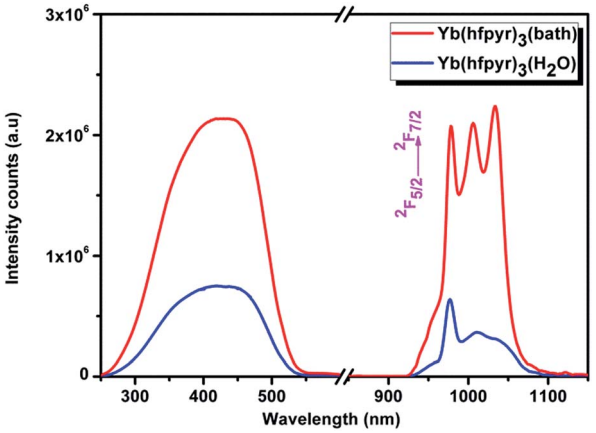

Fig. 8 Room temperature excitation and emission spectra of complexes 3 and 4 in the solid state.

ternary complex as compared to binary counterpart (Fig. S28 in ESI†).

Thus, the Yb^{3+} ion emission in the NIR region is important because in these regions biological tissues and fluids are relatively transparent, and the development of new Yb^{3+} ion complexes may find as bioprobes in fluoroimmunoassay and *in vivo* applications.[1a,33]

The excited state $^4F_{3/2}$ (Nd^{3+}) and $^2F_{5/2}$ (Yb^{3+}) lifetime values (τ_{obs}) of the Ln^{3+} complexes **1–4** were determined at ambient temperature (298 K), by monitoring within the intense lines of the $^4F_{3/2} \rightarrow {}^4I_{11/2}$ and $^2F_{5/2} \rightarrow {}^2F_{7/2}$ transitions, respectively (Fig. 9 and 10), and the pertinent values are given in Table 3. The observed luminescent decay profiles correspond to mono-exponential functions, highlighting the presence of single emissive Ln^{3+} center. The shorter lifetime values noted in the case of binary lanthanide complexes (**1** and **3**) may be due to the dominant non-radiative decay channels associated with the vibronic coupling due to the presence of solvent molecules in the coordination sphere of these respective complexes.[17b] On the other hand, a two-fold enhancement in the excited state

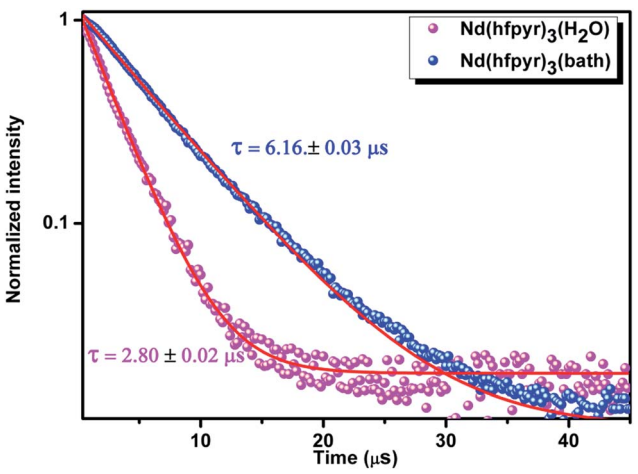

Fig. 9 Experimental luminescence decay profiles for complexes 1 and 2 in solid state monitored at approximately 1069 nm and excited 400 nm.

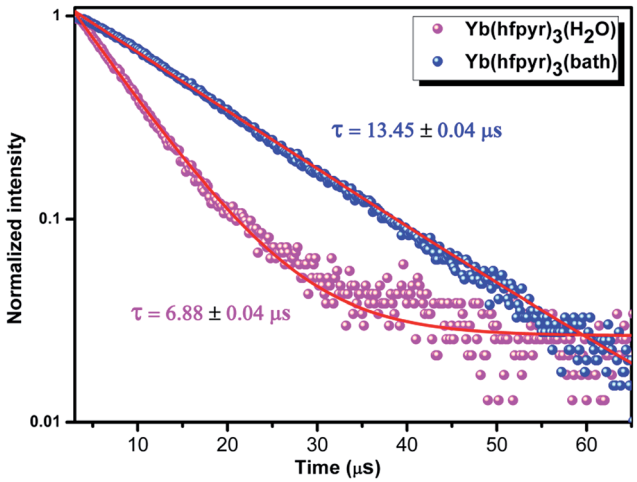

Fig. 10 Experimental luminescence decay profiles for complexes 3 and 4 in solid state monitored at approximately 979 nm and excited 400 nm.

lifetime values have been observed in the case of ternary Ln^{3+} complexes as compared to corresponding binary complexes.

The overall quantum yields ($\Phi_{overall}$) of the developed NIR emitting Nd^{3+} and Yb^{3+} complexes (**1–4**) have been calculated intending to understand more about the photophysical properties. Therefore, it is appropriate to analyse the NIR emission behaviour of the Ln^{3+} complexes in terms of overall quantum yields ($\Phi_{overall}$). As it is well-known that, the overall quantum yield is generally regulated by the sensitization efficiency of the antenna molecule (Φ_{sens}) as well as the intrinsic luminescent quantum yield (Φ_{Ln}) of the Ln^{3+} ion [$\Phi_{overall} = \Phi_{sens}\Phi_{Ln}$]. The Φ_{Ln} of the complexes was determined by using the following eqn (1).[2b,34]

$$\Phi_{Ln} = (\tau_{obs}/\tau_{rad}) \quad (1)$$

where τ_{obs} is the observed lifetime and τ_{rad} is 'natural' lifetime of Ln^{3+}. Table 3 summarizes the various photophysical properties of the Ln^{3+} complexes, such as $\Phi_{overall}$, Φ_{Ln}, and radiative (A_{RAD}) and non-radiative (A_{NR}) decay rates. The solid-state quantum yields ($\Phi_{overall}$) noted for the Nd^{3+} and Yb^{3+} ternary complexes (1.07 ± 0.05% for **2** and 3.08 ± 0.15% for **4**) are found to be significantly higher (2-fold) than that of the corresponding binary counterparts (0.45 ± 0.02% for **1** and 1.69 ± 0.08% for **3**). This can be explained on the basis of displacement of

Table 3 Luminescence parameters radiative (A_{RAD}, s^{-1}) and non-radiative (A_{NR}, s^{-1}) rates, lifetime (τ_{obs}, μs), intrinsic quantum yield (Φ_{Ln}, %) and overall quantum yield ($\Phi_{overall}$, %) for complexes **1–4**

Complex	A_{RAD} (s^{-1})	A_{NR} (s^{-1})	τ_{obs} (μs)	Φ_{Ln} (%)	$\Phi_{overall}$ (%)
$Nd(hfpyr)_3(H_2O)$ **1**	1607	3.65×10^5	2.80 ± 0.02	1.04	0.45
$Nd(hfpyr)_3$(bath) **2**	1737	1.61×10^5	6.16 ± 0.03	2.28	1.07
$Yb(hfpyr)_3(H_2O)$ **3**	2456	1.43×10^5	6.88 ± 0.04	0.34	1.69
$Yb(hfpyr)_3$(bath) **4**	2389	7.20×10^4	13.45 ± 0.04	0.67	3.08

potentially quenching O–H oscillators present in the coordination sphere of the metal ions by the ancillary ligand, 4,7-diphenyl-1,10-phenanthroline. Similar trends have been noted earlier.[4a,6b] These results are also in good agreement with the decrease of non-radiative decay rates in the corresponding ternary Ln^{3+} complexes. The luminescent lifetimes and quantum yields values observed in the present study are in line with, or moderately higher than the recently published results on NIR luminescent lanthanide β-diketonate complexes.[8g,h,10,35]

To calculate the efficiency of the sensitization process, it is necessary to know the radiative lifetime values (τ_{rad}), which are not easy to determine experimentally. It is clear from the literature that the τ_{rad} values for Nd^{3+} and Yb^{3+} vary widely and depend heavily on the solvent or the physical state of the sample. Taking into account 0.27 ms for Nd^{3+} as and a value of 2.0 ms commonly assumed for Yb^{3+}, the data for sensitization Φ_{sens} = 0.45 for Nd^{3+}, while a value >1 is noted for Yb^{3+}, meaning that the actual radiative lifetime is larger than 2 ms in our system. Similar kind of results has also been reported by Bünzli and co-workers.[7c]

Synthesis, characterization and photophysical properties of PMMA doped hybrid materials

In view of the low cost, low optical absorbance and good mechanical properties,[10] in the present study PMMA has been blended with the developed NIR emitting Yb^{3+} ternary complex (**4**) in proportions of 1, 3, 5, 7 and 9% (w/w) and corresponding polymeric films [PMMA@1% Yb, PMMA@3% Yb, PMMA@5% Yb, PMMA@7% Yb and PMMA@9% Yb] were isolated, characterized and evaluated their photophysical properties. The FT-IR spectra of precursor metal complex $Yb(hfpyr)_3(bath)$ **4** and the corresponding embedded Yb^{3+} complex in PMMA film (PMMA@7% Yb) were recorded in the 400–4000 cm^{-1} region and the results are shown in Fig. S29 in ESI.†

The characteristic absorptions of the $-O-CH_2$ asymmetric stretch, the $-CH_3$ asymmetric stretch, the –C═O stretch, the $-O-CH_3$ deformation and the –C–O–C– symmetric stretch of pure PMMA was observed at 3000–3002, 2947–2950, 1730–1732, 1380–1385 and 989–993 cm^{-1} region, respectively.[36] On the other hand, the weakening of vibrations of the ternary complex along with PMMA absorptions noted in the hybrid film indicate that the metal complex is embedded into PMMA matrix. The thermal stabilities of the precursor complex $Yb(hfpyr)_3(bath)$ **4** as well as the typical metal complex embedded into polymer film (PMMA@7% Yb) have been assessed by TGA and DTA analyses and the results are depicted in Fig. S24 and S30 respectively in ESI.† As can be clearly seen from the DTA results that the thermal stability of the parent Yb^{3+} ternary complex (366 °C decomposition temperature) was significantly improved after doping into the PMMA matrix (416 °C decomposition temperature). The TGA curve of PMMA@7% Yb film indicates that the decomposition starts at 290 °C. The polymer has been completely departed from the hybrid material when the temperature reaches at 427 °C.

The solid-state excitation and the emission profiles of a series of PMMA embedded Yb ternary metal complex [PMMA@1% Yb, PMMA@3% Yb, PMMA@5% Yb, PMMA@7% Yb and PMMA@9% Yb] polymeric films recorded at room temperature (298 K) are displayed in Fig. 11. A broad band noted in the wavelength region 250–500 nm of the excitation spectra can be attributed to the absorptions of the ligand systems. The emission spectra (λ_{exc} = 400 nm) clearly illustrates the presence of characteristic emission band of Yb^{3+} ion at 979 nm, which can be assigned to $^2F_{5/2} \rightarrow {}^2F_{7/2}$ transition.[6c,34] Further, the luminescence intensity of the Yb^{3+} ion at 979 nm increases initially with the increase of dopant metal complex concentration in the polymer film to a maximum (PMMA@7% Yb) and thereafter decreases at higher concentration (PMMA@9% Yb). The energy transfer between the Yb^{3+} ions themselves is a non-radiative process, which accounts for the observed decrease in the Yb^{3+} emission, especially at high dopant metal complex concentration. It is noteworthy to mention that the emission intensity of the 7% Yb complex doped PMMA film at 979 nm has been markedly improved (about 1.4 fold) as compared to the precursor ternary Yb^{3+} complex. As a consequence, the overall quantum yields of the hybrid materials (3.40–3.62%) have also been moderately enhanced (Table 4). In conclusion, the above results disclose that Yb^{3+} ternary complex retains its original photophysical properties even after doping into the PMMA matrix. Further, the thermal stability and film forming properties have been significantly improved as compared to precursor complex.

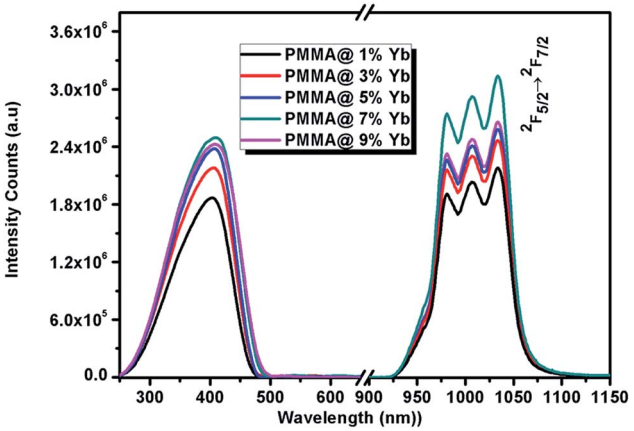

Fig. 11 Excitation and emission spectra of PMMA films doped with 1, 3, 5, 7 and 9% (w/w) of $Yb(hfpyr)_3(bath)$. The data were recorded at 298 K.

Table 4 Luminescence parameters for complex **4** and PMMA films doped with various amounts of the complex **4**, at 298 K

Complex/film	A_{RAD} (s^{-1})	A_{NR} (s^{-1})	τ_{obs} (μs)	Φ_{Ln} (%)	$\Phi_{overall}$ (%)
$Yb(hfpyr)_3(bath)$	2289	7.20×10^4	13.45 ± 0.02	0.743	3.08
PMMA@1% Yb	2259	6.50×10^4	14.87 ± 0.02	0.738	3.36
PMMA@3% Yb	2317	6.54×10^4	14.76 ± 0.02	0.728	3.42
PMMA@5% Yb	2443	6.61×10^4	14.57 ± 0.02	0.744	3.56
PMMA@7% Yb	2432	6.47×10^4	14.88 ± 0.02	0.741	3.62
PMMA@9% Yb	2388	6.50×10^4	14.82 ± 0.02	0.743	3.54

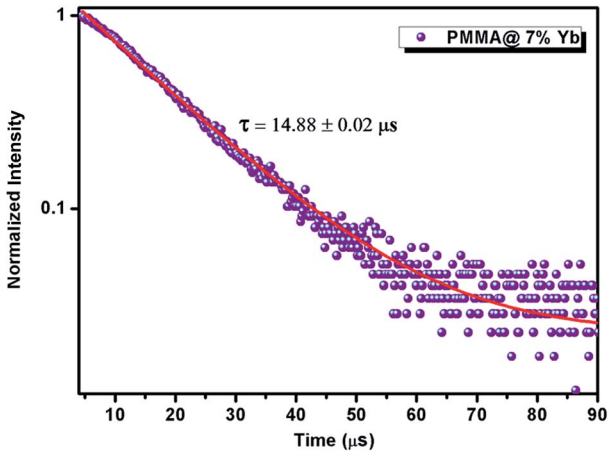

Fig. 12 Experimental luminescence decay profiles of PMMA film@7% (w/w) of Yb(hfpyr)$_3$(bath) monitored at approximately 975 nm and excited 400 nm.

The luminescent decay profiles of the polymeric hybrid films were obtained by monitoring the emission at 979 nm corresponding to $^2F_{5/2} \rightarrow {}^2F_{7/2}$ transition and excited at 400 nm and the results are given in Fig. 12 and S31.† The life time values of the isolated hybrid films are listed in Table 2. All the τ values of the hybrid polymer films (14–15 μs) are found to be moderately higher than the precursor Yb^{3+} ternary complex **4** (13.45 μs), thus highlighting the radiative process are operative in the doped films due to the absence of multiphonon relaxation by coupling with the –OH oscillators.[9] Furthermore, the excited state lifetime values are not influenced by the doping process into the PMMA matrix.

Conclusions

In summary, a novel β-diketonate ligand, 4,4,5,5,6,6,6-heptafluoro-3-hydroxy-1-(pyren-1-yl)hex-2-en-1-one has been successfully synthesized by incorporating highly conjugated pyrene moiety as a sensitizing unit and polyfluorinated alkyl group with low energy C–F oscillators, with an aim to develop near-infrared (NIR) emitting lanthanide complexes. Notably, the designed β-diketonate ligand has a triplet energy level of 16 207 cm^{-1}, which lies well above the energy of the main emitting level of Nd^{3+} ($^4F_{3/2}$ = 11 257 cm^{-1}) or Yb^{3+} ($^2F_{5/2}$ = 10 400 cm^{-1}), implying that it can act as an efficient antenna molecule for the sensitization of NIR emitting lanthanide ions. Further, the developed NIR emitting lanthanide complexes possess markedly high molar absorption coefficient values (about ε = 49 000 to 50 000 L mol^{-1} cm^{-1}), indicating the adequate light-harvesting capacity of these compounds. The luminescent lifetimes and quantum yields values observed in the present study are found be significantly higher than many of the existing NIR emitting lanthanide β-diketonate complexes. Thus, the currently derived new Nd^{3+} and Yb^{3+} compounds may find potential applications as bioprobes in fluoroimmunoassay and new optical amplification materials for telecommunications. It is interesting to note that the thermal stability of the Yb^{3+} ternary complex incorporated PMMA film has been greatly enhanced as compared to parent compound, apart from exhibiting good film forming capacity.

Acknowledgements

One of the authors T. M. George thanks UGC, New Delhi for the award of Senior Research Fellowship.

References

1 (*a*) S. Comby and J.-C. G. Bünzli, in *Handbook on the Physics and Chemistry of Rare Earths*, ed. K. A. Gschneidner, J.-C. G. Bünzli and K. P. Vitalij, Elsevier, 2007, vol. 37, pp. 217–470; (*b*) J.-C. G. Bünzli and S. V. Eliseeva, *Chem. Sci.*, 2013, **4**, 1939; (*c*) S. V. Eliseeva and J.-C. G. Bünzli, *Chem. Soc. Rev.*, 2010, **39**, 189–227; (*d*) A. J. Amoroso and S. J. A. Pope, *Chem. Soc. Rev.*, 2015, **44**, 4723–4742; (*e*) J. C. G. Bünzli and S. V. Eliseeva, *J. Rare Earths*, 2010, **28**, 824–842; (*f*) L. Prodi, E. Rampazzo, F. Rastrelli, A. Speghini and N. Zaccheroni, *Chem. Soc. Rev.*, 2015, **44**, 4922–4952.

2 (*a*) P. A. Tanner and C.-K. Duan, *Coord. Chem. Rev.*, 2010, **254**, 3026–3029; (*b*) J. Feng and H. Zhang, *Chem. Soc. Rev.*, 2013, **42**, 387–410; (*c*) L. Armelao, S. Quici, F. Barigelletti, G. Accorsi, G. Bottaro, M. Cavazzini and E. Tondello, *Coord. Chem. Rev.*, 2010, **254**, 487–505; (*d*) J.-C. G. Bünzli and C. Piguet, *Chem. Soc. Rev.*, 2005, **34**, 1048–1077.

3 (*a*) X. Wang, H. Chang, J. Xie, B. Zhao, B. Liu, S. Xu, W. Pei, N. Ren, L. Huang and W. Huang, *Coord. Chem. Rev.*, 2014, **273–274**, 201–212; (*b*) J.-C. G. Bünzli, *Acc. Chem. Res.*, 2006, **39**, 53–61; (*c*) M. L. P. Reddy and S. Sivakumar, *Dalton Trans.*, 2013, **42**, 2663–2678; (*d*) E. G. Moore, A. P. S. Samuel and K. N. Raymond, *Acc. Chem. Res.*, 2009, **42**, 542–552.

4 (*a*) A. D. Bettencourt-dias, P. S. Barber and S. Viswanathan, *Coord. Chem. Rev.*, 2014, **273–274**, 165–200; (*b*) D. V. Kazakov and F. E. Safarov, *Photochem. Photobiol. Sci.*, 2014, **13**, 1646–1649; (*c*) M. L. P. Reddy, V. Divya and R. Pavithran, *Dalton Trans.*, 2013, **42**, 15249–15262; (*d*) Y. Ma and Y. Wang, *Coord. Chem. Rev.*, 2010, **254**, 972–990.

5 (*a*) K. Binnemans, in *Handbook on the Physics and Chemistry of Rare Earths*, ed. J.-C. G. B. Karl, A. Gschneidner and K. P. Vitalij, Elsevier, 2005, vol. 35, pp. 107–272; (*b*) D. B. A. Raj, B. Francis, M. L. P. Reddy, R. R. Butorac, V. M. Lynch and A. H. Cowley, *Inorg. Chem.*, 2010, **49**, 9055–9063; (*c*) T. M. George, M. J. Sajan, N. Gopakumar and M. L. P. Reddy, *J. Photochem. Photobiol., A*, 2016, **317**, 88–99; (*d*) J. Sun, B. Song, Z. Ye and J. Yuan, *Inorg. Chem.*, 2015, **54**, 11660–11668; (*e*) T. V. Usha Gangan and M. L. P. Reddy, *Dalton Trans.*, 2015, **44**, 15924–15937; (*f*) F. Cao, Z. Yuan, J. Liu and J. Ling, *RSC Adv.*, 2015, **5**, 102535–102541; (*g*) P. N. Remya, S. Biju, M. L. Reddy, A. H. Cowley and M. Findlater, *Inorg. Chem.*, 2008, **47**, 7396–7404; (*h*) S. Biju, D. B. A. Raj, M. L. P. Reddy and B. M. Kariuki, *Inorg. Chem.*, 2006, **45**, 10651–10660; (*i*) B. Francis, C. Heering, R. O. Freire, M. L. P. Reddy and C. Janiak, *RSC Adv.*, 2015, **5**, 90720–90730; (*j*) K. Miyata, Y. Konno, T. Nakanishi, A. Kobayashi, M. Kato, K. Fushimi

and Y. Hasegawa, *Angew. Chem., Int. Ed.*, 2013, **52**, 6413–6416; (*k*) J. Yuasa, T. Ohno, H. Tsumatori, R. Shiba, H. Kamikubo, M. Kataoka, Y. Hasegawa and T. Kawai, *Chem. Commun.*, 2013, **49**, 4604–4606; (*l*) Y. Hirai, T. Nakanishi, Y. Kitagawa, K. Fushimi, T. Seki, H. Ito, H. Fueno, K. Tanaka, T. Satoh and Y. Hasegawa, *Inorg. Chem.*, 2015, **54**, 4364–4370; (*m*) P. P. Lima, M. M. Nolasco, F. A. A. Paz, R. A. S. Ferreira, R. L. Longo, O. L. Malta and L. D. Carlos, *Chem. Mater.*, 2013, **25**, 586–598; (*n*) V. Divya, R. O. Freire and M. L. Reddy, *Dalton Trans.*, 2011, **40**, 3257–3268; (*o*) V. Divya, V. Sankar, K. G. Raghu and M. L. P. Reddy, *Dalton Trans.*, 2013, **42**, 12317–12323.

6 (*a*) C. Yu, Z. Zhang, L. Liu, H. Li, Y. He, X. Lu, W.-K. Wong and R. A. Jones, *New J. Chem.*, 2015, **39**, 3698–3707; (*b*) Y. Hou, J. Shi, W. Chu and Z. Sun, *Eur. J. Inorg. Chem.*, 2013, **7**, 3063–3069; (*c*) Z. Zhang, C. Yu, L. Liu, H. Li, Y. He, X. Lü, W. K. Wong and R. A. Jones, *J. Photochem. Photobiol., A*, 2016, **314**, 104–113.

7 (*a*) S. Comby, D. Imbert, C. Vandevyver and J. C. Bünzli, *Chemistry*, 2007, **13**, 936–944; (*b*) N. M. Shavaleev, R. Scopelliti, F. Gumy and J. C. Bünzli, *Inorg. Chem.*, 2008, **47**, 9055–9068; (*c*) S. Comby, D. Imbert, A. S. Chauvin and J. C. G. Bünzli, *Inorg. Chem.*, 2006, **45**, 732–743; (*d*) E. R. Trivedi, S. V. Eliseeva, J. Jankolovits, M. M. Olmstead, S. Petoud and V. L. Pecoraro, *J. Am. Chem. Soc.*, 2014, **136**, 1526–1534; (*e*) A. Sanguineti, A. Monguzzi, G. Vaccaro, F. Meinardi, E. Ronchi, M. Moret, U. Cosentino, G. Moro, R. Simonutti, M. Mauri, R. Tubino and L. Beverina, *Phys. Chem. Chem. Phys.*, 2012, **14**, 6452; (*f*) S. Dang, J. B. Yu, X. F. Wang, Z. Y. Guo, L. N. Sun, R. P. Deng, J. Feng, W. Q. Fan and H. J. Zhang, *J. Photochem. Photobiol., A*, 2010, **214**, 152–160; (*g*) X. S. Ke, B. Y. Yang, X. Cheng, S. L. F. Chan and J. L. Zhang, *Chem.–Eur. J.*, 2014, **20**, 4324–4333; (*h*) P. B. Glover, A. P. Bassett, P. Nockemann, B. M. Kariuki, R. Van Deun and Z. Pikramenou, *Chem.–Eur. J.*, 2007, **13**, 6308–6320.

8 (*a*) A. W. Woodward, A. Frazer, A. R. Morales, J. Yu, A. F. Moore, A. D. Campiglia, E. V. Jucov, T. V. Timofeeva and K. D. Belfield, *Dalton Trans.*, 2014, **43**, 16626–16639; (*b*) P. Martín-Ramos, P. S. Pereira da Silva, V. Lavín, I. R. Martín, F. Lahoz, P. Chamorro-Posada, M. Ramos Silva and J. Martín-Gil, *Dalton Trans.*, 2013, **42**, 13516–13526; (*c*) L. Yang, Z. Gong, D. Nie, B. Lou, Z. Bian, M. Guan, C. Huang, H. J. Lee and W. P. Baik, *New J. Chem.*, 2006, **30**, 791–796; (*d*) A. Monguzzi, R. Tubino, F. Meinardi, A. O. Biroli, M. Pizzotti, F. Demartin, F. Quochi, F. Cordella and M. A. Loi, *Chem. Mater.*, 2009, **21**, 128–135; (*e*) X. Guo, H. Guo, L. Fu, L. D. Carlos, R. A. S. Ferreira, L. Sun, R. Deng and H. Zhang, *J. Phys. Chem. C*, 2009, **113**, 12538–12545; (*f*) T. S. Kang, B. S. Harrison, M. Bouguettaya, T. J. Foley, J. M. Boncella, K. S. Schanze and J. R. Reynolds, *Adv. Funct. Mater.*, 2003, **13**, 205–210; (*g*) Z. Ahmed and K. Iftikhar, *J. Phys. Chem. A*, 2013, **117**, 11183–11201; (*h*) N. M. Shavaleev, R. Scopelliti, F. Gumy and J. C. G. Bünzli, *Eur. J. Inorg. Chem.*, 2008, **9**, 1523–1529; (*i*) B. L. Reid, S. Stagni, J. M. Malicka, M. Cocchi, A. N. Sobolev, B. W. Skelton, E. G. Moore, G. S. Hanan, M. I. Ogden and M. Massi, *Chem.–Eur. J.*, 2015, **21**, 18354–18363.

9 (*a*) G. M. Davies, R. J. Aarons, G. R. Motson, J. C. Jeffery, H. Adams, S. Faulkner and M. D. Ward, *Dalton Trans.*, 2004, 1136–1144, DOI: 10.1039/b400992d; (*b*) J. Feng, J.-B. Yu, S.-Y. Song, L.-N. Sun, W.-Q. Fan, X.-M. Guo, S. Dang and H.-J. Zhang, *Dalton Trans.*, 2009, 2406, DOI: 10.1039/b819644c; (*c*) N. M. Shavaleev, S. J. A. Pope, Z. R. Bell, S. Faulkner and M. D. Ward, *Dalton Trans.*, 2003, 808–814, DOI: 10.1039/b300294b.

10 S. Biju, Y. K. Eom, J.-C. G. Bünzli and H. K. Kim, *J. Mater. Chem. C*, 2013, **1**, 6935–6944.

11 B. Li, H. Li, P. Chen, W. Sun, C. Wang, T. Gao and P. Yan, *Phys. Chem. Chem. Phys.*, 2015, **17**, 30510–30517.

12 (*a*) A. J. Howarth, M. B. Majewski and M. O. Wolf, *Coord. Chem. Rev.*, 2015, **282–283**, 139–149; (*b*) A. G. Crawford, A. D. Dwyer, Z. Q. Liu, A. Steffen, A. Beeby, L. O. Palsson, D. J. Tozer and T. B. Marder, *J. Am. Chem. Soc.*, 2011, **133**, 13349–13362.

13 (*a*) R. Haldar, K. Prasad, P. K. Samanta, S. Pati and T. K. Maji, *Cryst. Growth Des.*, 2016, **16**, 82–91; (*b*) F. Liu, C. Tang, Q. Q. Chen, F. F. Shi, H. B. Wu, L. H. Xie, B. Peng, W. Wei, Y. Cao and W. Huang, *J. Phys. Chem. C*, 2009, **113**, 4641–4647; (*c*) C. Tang, F. Liu, Y. J. Xia, J. Lin, L. H. Xie, G. Y. Zhong, Q. L. Fan and W. Huang, *Org. Electron.*, 2006, **7**, 155–162; (*d*) C. Tang, F. Liu, Y.-J. Xia, L.-H. Xie, A. Wei, S.-B. Li, Q.-L. Fan and W. Huang, *J. Mater. Chem.*, 2006, **16**, 4074.

14 J. E. Sohna Sohna and F. Fages, *Tetrahedron Lett.*, 1997, **38**, 1381–1384.

15 S. Faulkner, M. C. Carrie, S. J. A. Pope, J. Squire, A. Beeby and P. G. Sammes, *Dalton Trans.*, 2004, 1405–1409, DOI: 10.1039/b401302f.

16 S. J. A. Pope, *Polyhedron*, 2007, **26**, 4818–4824.

17 (*a*) Y. Hasegawa, T. Ohkubo, K. Sogabe, Y. Kawamura, Y. Wada, N. Nakashima and S. Yanagida, *Angew. Chem., Int. Ed.*, 2000, **39**, 357–360; (*b*) A. Døssing, *Eur. J. Inorg. Chem.*, 2005, **2005**, 1425–1434; (*c*) A. Beeby, I. M. Clarkson, R. S. Dickins, S. Faulkner, D. Parker, L. Royle, A. S. de Sousa, J. A. Gareth Williams and M. Woods, *J. Chem. Soc., Perkin Trans. 2*, 1999, 493–504, DOI: 10.1039/a808692c.

18 (*a*) J. Li, H. Li, P. Yan, P. Chen, G. Hou and G. Li, *Inorg. Chem.*, 2012, **51**, 5050–5057; (*b*) D. B. A. Raj, S. Biju and M. L. P. Reddy, *J. Mater. Chem.*, 2009, **19**, 7976–7983.

19 (*a*) D. B. Ambili Raj, S. Biju and M. L. Reddy, *Dalton Trans.*, 2009, **36**, 7519–7528; (*b*) V. Divya and M. L. P. Reddy, *J. Mater. Chem. C*, 2013, **1**, 160–170; (*c*) D. B. A. Raj, S. Biju and M. L. P. Reddy, *Inorg. Chem.*, 2008, **47**, 8091–8100.

20 (*a*) W. Fan, J. Feng, S. Song, Y. Lei, L. Zhou, G. Zheng, S. Dang, S. Wang and H. Zhang, *Nanoscale*, 2010, **2**, 2096–2103; (*b*) Z. Zhang, W. Feng, P. Su, X. Lü, J. Song, D. Fan, W. K. Wong, R. A. Jones and C. Su, *Inorg. Chem.*, 2014, **53**, 5950–5960.

21 W. Li, P. Yan, G. Hou, H. Li and G. Li, *RSC Adv.*, 2013, **3**, 18173–18180.

22 (*a*) K. S. Bejoymohandas, A. Kumar, S. Sreenadh, E. Varathan, S. Varughese, V. Subramanian and

M. L. P. Reddy, *Inorg. Chem.*, 2016, **55**, 3448–3461; (*b*) K. S. Bejoymohandas, A. Kumar, S. Varughese, E. Varathan, V. Subramanian and M. L. P. Reddy, *J. Mater. Chem. C*, 2015, **3**, 7405–7420.

23 S. V. Eliseeva, D. N. Pleshkov, K. A. Lyssenko, L. S. Lepnev, J. C. Bünzli and N. P. Kuzmina, *Inorg. Chem.*, 2010, **49**, 9300–9311.

24 J. A. Cunningham, D. E. Sands, W. F. Wagner and M. F. Richardson, *Inorg. Chem.*, 1969, **8**, 22–28.

25 S. Biju, M. L. P. Reddy, A. H. Cowley and K. V. Vasudevan, *Cryst. Growth Des.*, 2009, **9**, 3562–3569.

26 V. Divya, S. Biju, R. L. Varma and M. L. P. Reddy, *J. Mater. Chem.*, 2010, **20**, 5220–5227.

27 A. R. Ramya, D. Sharma, S. Natarajan and M. L. P. Reddy, *Inorg. Chem.*, 2012, **51**, 8818–8826.

28 F. J. Steemers, W. Verboom, D. N. Reinhoudt, E. B. van der Tol and J. W. Verhoeven, *J. Am. Chem. Soc.*, 1995, **117**, 9408–9414.

29 L. Yang, Z. Gong, D. Nie, B. Lou, Z. Bian, M. Guan, C. Huang, H. J. Lee and W. P. Baik, *New J. Chem.*, 2006, **30**, 791–796.

30 O. L. Malta, H. F. Brito, J. F. S. Menezes, F. R. Gonçalves e Silva, C. de Mello Donegá and S. Alves Jr, *Chem. Phys. Lett.*, 1998, **282**, 233–238.

31 (*a*) P. O. Alink, S. I. Klink, L. Grave, F. G. A. Peters, J. W. Hofstraat, F. Geurts and F. C. J. M. van Veggel, *J. Chem. Soc., Perkin Trans. 2*, 2001, 363–372; (*b*) W.-T. Wong and W. P.-W. Lai, *New J. Chem.*, 2000, **24**, 943–944; (*c*) F. C. J. M. van Veggel and J. W. Stouwdam, *Nano Lett.*, 2002, **2**, 733–737; (*d*) L. N. Sun, J. B. Yu, G. L. Zheng, H. J. Zhang, Q. G. Meng, C. Y. Peng, L. S. Fu, F. Y. Liu and Y. N. Yu, *Eur. J. Inorg. Chem.*, 2006, **19**, 3962–3973; (*e*) J.-C. G. Bünzli and S. V. Eliseeva, *Springer Ser. Fluoresc.*, 2011, 1–45, DOI: 10.1007/4243.

32 O. L. Malta, F. R. Goncalves e Silva, C. Reinhard, H.-U. Güdel, C. Piguet, J. E. Moser and J.-C. G. Bünzli, *J. Phys. Chem. A*, 2002, **106**, 1670–1677.

33 R. J. Aarons, G. M. Davies, G. R. Motson, J. C. Jeffery, H. Adams, S. Faulkner and M. D. Ward, *Dalton Trans.*, 2004, 1136–1144.

34 (*a*) L. D. Carlos, R. A. S. Ferreira, V. D. Bermudez and S. J. L. Ribeiro, *Adv. Mater.*, 2009, **21**, 509–534; (*b*) A. de Bettencourt-Dias, *Dalton Trans.*, 2007, 2229–2241, DOI: 10.1039/b702341c.

35 (*a*) L. N. Puntus, K. J. Schenk and J.-C. G. Bünzli, *Eur. J. Inorg. Chem.*, 2005, **2005**, 4739–4744; (*b*) Y. F. Yuan, T. Cardinaels, K. Lunstroot, K. Van Hecke, L. Van Meervelt, C. Görller-Walrand, K. Binnemans and P. Nockemann, *Inorg. Chem.*, 2007, **46**, 5302–5309.

36 P. Y. Weizuo Li, G. Hou, H. Li and G. Li, *Dalton Trans.*, 2013, **42**, 11537–11547.

